Scientia Iranica A (2023) 30(6), 1911–1924

Sharif University of Technology
Scientia Iranica
Transactions A: Civil Engineering
http://scientiairanica.sharif.edu

Field and laboratory investigations of the effective contact surface between sleeper and ballast particles in railway tracks

H. Refahiat-Nikoo[a], J.-A. Zakeri[b,*], and S. Mohammadzadeh[a]

a. *School of Railway Engineering, Iran University of Science and Technology, Tehran, Iran.*
b. *Center of Excellence in Railway Transportation, School of Railway Engineering, Iran University of Science and Technology, Tehran, Iran.*

Received 15 December 2021; received in revised form 10 May 2022; accepted 5 December 2022

KEYWORDS
Effective contact surface;
USP;
Ballast particles;
Ballast box test;
Sensitive pressure paper.

Abstract. Ballast is a porous layer that reduces the effective contact surface between sleeper and ballast layer. This paper uses laboratory and field tests to measure the contact surface between sleeper and ballast. In field experiments, by installing sensitive papers under the sleepers of a track, the cyclic load was imposed by passing trains. After passing a certain amount of load, the sensitive pressure paper was removed and the contact surface was measured, while in the laboratory investigation, the ballast box test was used to achieve a similar goal. The values obtained for the contact surfaces showed that the contact areas with 200 kN axle load were about 4.9% and 8.1% for concrete and wooden sleepers, respectively, and this value increases with increasing axle load and load cycle. The average contact surface for 30, 37.7, and 45.2 kN is 3.8%, 4.5%, and 5.1%, respectively. The average contact area for 6700, 20000, and 50000 cycles is 4.2%, 4.6%, and 4.7%, respectively. The average contact area for ballast type 1 was 4.6%, for ballast type 4 was 5.5%, and for the sample of ballast from the field test site was 5.3%. The results showed that the effective contact areas between the sleeper and the ballast were 21.6% and 15.9% for soft and stiff Under Sleeper Pads (USPs), respectively.

1. Introduction

Ballast is a commonly used material for transportation infrastructure. In a railway substructure, loads are applied on the rails and transferred through sleepers to the ballast. Under long-term repeated train loadings, ballast may experience flow and other deterioration, which in turn will change the stress distributions within the ballast and between the ballast and sleepers [1]. The sleeper/ballast interface is an essential stage in the transfer of train loads from a railway track structure into the ground. Generally, only a small number of ballast grains support the sleeper base. The resulting localized contact stresses can be very high, especially for modern concrete sleepers on hard igneous ballast. This may result in damage to both sleepers and ballast and reduce the stability of the interface [2].

The contact surface between the ballast layer and the sleeper is not uniform and smooth. The presence of empty spaces between ballast particles reduces the effective contact surface between the sleeper and ballast. On the other hand, the effective contact surface of the

*. *Corresponding author.*
E-mail addresses: hamidreza.nikoo72@gmail.com (H. Refahiat-Nikoo); zakeri@iust.ac.ir (J.-A. Zakeri)

doi: 10.24200/sci.2022.59574.6315

sleeper and ballast is important because if the contact surface increases due to the ballast particle crushing, the track will change from the elastic to the rigid body, and damaging the adjacent structures. However, increasing dynamic stresses from the passage of trains progressively degrades and fouls the primary load-bearing ballast layer, inevitably leading to excessive settlement and instability, damage to track elements, and more frequent maintenance. Ballasted tracks are subjected to even greater stress and faster deterioration in sections where the reduced ballast thickness is used (e.g., bridge decks) or at locations where heavier concrete sleepers are used instead of light-weight timber sleepers. The inclusion of Under Sleeper Pads (USPs) at the base of a concrete sleeper is one measure used to minimize dynamic stresses and subsequent track deterioration [3].

The contact surface between the sleeper and ballast is much lower in reality. This research investigated the contact surface between ballast and wooden and B70 concrete sleepers used in Iran. The purpose of this investigation and experimentation is to develop a complete understanding of the mechanical behavior of the contact surface between sleeper and ballast and its changes according to the materials used and the speed of loading. The change of materials is studied to investigate how the change of ballast and sleeper type changes the contact surface size and the effect of loading speed on the sleeper and ballast contact surface. Understanding these behaviors and the size of the contact surface will help understand the track's stiffness and prevent the damage caused by the variation of track stiffness. The gap between previous studies was the difference in the value obtained for the contact surface between the sleeper and the ballast, and this study was conducted to clarify the issue.

Due to the importance of the sleeper-ballast contact surface and the pressure distribution between them, many researchers have studied this subject with different methods such as Indraratna and Salim [4] in 2005, Esveld [5] in 2001, Selig and Waters [6] in 1994, and Lichtberger [7] in 2007. Some researchers have investigated stress distribution between sleeper and ballast including Talbot [8] from 1918 to 1940, to measure stress on railway tracks, and they also discussed the challenges of measuring pressure on the sleeper and ballast contact surface. Many researchers have done numerical studies using Discrete Element Modelling (DEM) to determine the forces and interaction between ballast and sleeper [9–12]. Ferro et al. investigated the effect of sleeper material on track behavior in 2020 [13]. The effect of USP has been studied in previous articles [14–16].

In 2007, Zakeri and Sadeghi [17] conducted field studies of stress distribution under a B70 concrete sleeper and obtained real stress distribution under sleepers. In 1986, Profillidis and Poniridis [18] investigated the mechanical behavior at the sleeper and ballast interface. Hen [19] studied the effective contact surface in 1978 at the University of Graz, Austria and obtained the percentage of contact area between sleepers and ballast ranging from 4 to 10% and 1 to 9% for the wooden and prefabricated concrete sleepers, respectively; however, in the case of new tracks, they found the contact area to be between 0.5 and 3%. In 2021, Sysyn et al. studied the mechanism of the dynamic impact of sleeper and ballast in the void zone [20]. Jing et al. [21] studied the contribution of ballast layer components to the lateral resistance of ladder sleeper track. The sleeper-ballast interface of railway tracks is directly associated with lateral resistance, which plays an important role in the mechanical behavior of ballasted tracks. The application of winged and frame sleepers was another innovative idea proposed by Jing et al. [22]. By using this method, the contact surface increases, hence high lateral resistance. Many studies have investigated the lateral resistance of railway tracks [23–25].

The most recent research was conducted in 2013 by McHenry [26] who used surface measurement sensors to measure the contact area and pressure distribution between concrete sleepers and ballast and then, provided different percentages for various ballast types. Figure 1 illustrates the details of this test.

The values of the contact surface between ballast and sleeper are acquired using the ballast box experiment and field studies, as shown in Tables 1 and 2.

Furthermore, Abadi et al. [27] performed experi-

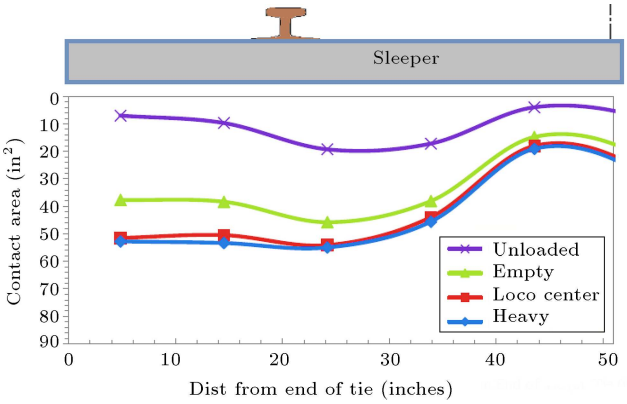

Figure 1. Chart of contact surface between sleeper and ballast.

Table 1. Ballast box test results.

	Average contact area	
Ballast layer	**10kips load**	**20kips load**
Fouled	34.51%	40.9%
Moderate	29.38%	32.9%
New	16.77%	20.4%

Table 2. Field test results.

Zone	Axle load			
	Unloaded	Empty	Loco	Heavy
Mod. ballast	13.3%	35.7%	42%	43%
New ballast	7.4%	21.9%	29.6%	31.2%
Fouled ballast	2.5%	28.4%	37.7%	39.7%

ments to measure the contact surface between sleeper and ballast to record sleeper loading history, which was in contact with ballast particles that experienced over 3 million loading cycles by using pressure paper. The results of this research are summarized in Table 3.

2. Methodology

The ballast is the first layer that receives the load transmitted to the lower layers from the sleeper. Transmission of the vertical loads from the rails to the sleeper results in extensive contact pressure on the bottom surface of the sleeper, which is equal to the load applied by the wheels in the opposite direction and represents the reaction of the ballast layer against the loads transferred from the sleeper. Figure 2 shows an example of the stress distribution on the ballast layer.

Determining the shape and distribution of this pressure beneath the sleepers depends on several factors, such as shape, type, materials of sleepers, ballast density, the axle load of the track, sleeper mechanical properties (rigidity), quality of railway maintenance, the volume of traffic, the elapsed time since tamping, and quality of ballast materials. The contact pressure surface between the sleeper and ballast occurs beneath rail seats when the ballast is tamped. However, after a period of train operation, the distribution of contact pressure between the sleepers and ballast shifts to a uniform distribution. It is, therefore, easy to see that the distribution of contact pressure between the sleeper and ballast is time dependent. This is why some researchers justify and prescribe a uniform distribution of stress under sleepers. Therefore, when the track maintenance is not done on time, the stress distribution is more uniform and therefore, the amount of bending stress in the middle of the sleeper increases. Thus, to prevent the increase in bending stress in the middle

Table 3. Results obtained for the experiments.

Sleeper type	Test ID	Percentage contact area per sleeper, 10–50 MPa pressure paper	Average contact pressure, MPa calculated as $F_{max}/A_{contact}$	Notes
Mono-block	Case 1	0.18	76.5	Increasing finer proportion
	Case 2	0.38	36.2	
	Case 3	0.63	21.9	
	TLB	0.52	26.5	Two-layered
	RPS	0.2	68.8	NR
	Stiff USP	1.64	8.4	Stiff
	Soft USP	1.05	13.1	Soft
Plastic	NR	3.08	4.9	NR
Wooden	NR	1.56	9.7	

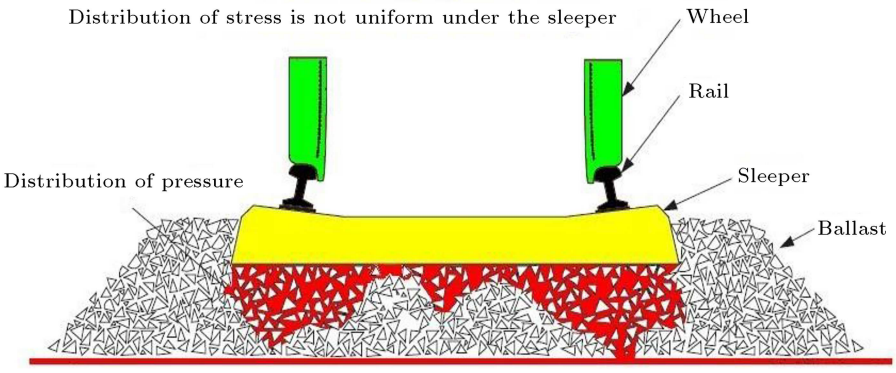

Figure 2. The actual stress distribution under the sleeper.

Figure 3. Sensitive pressure paper used.

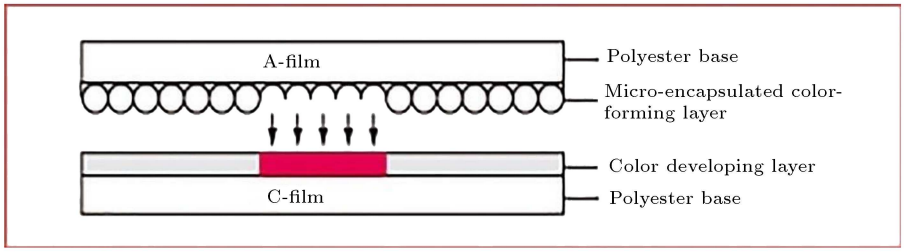

Figure 4. How pressure paper works.

of the sleeper, the ballast is tamped under the rail seat. If the stress distribution under the sleeper is not uniform, the surface under the sleeper, which effectively transmits stresses and forces to the ballast layer, should be determined. This surface is known as the effective surface [28].

3. Measuring instruments

In this study, a pressure paper was used to measure the contact area between the sleeper and the ballast. The pressure paper has a thin membrane comprising colored microcapsule and color-developing materials. The microcapsules in the color-forming layer are broken by pressure, and the colorless dye is absorbed into the developer, causing a chemical reaction to produce a red color. The microcapsules containing the color-forming material are adjusted to varying sizes and strengths and are coated uniformly, producing a color density corresponding to the amount of pressure. Its properties are described in detail by Fuji Film [29]. Pressure paper, when pressed, changes its color to red according to the intensity of the pressure that is applied. The pressure paper is composed of two polyester bases, A-Film and C-Film. A-Film is coated with a micro-encapsulated color-forming material, and a C-Film is coated with a color-developing material. A-Film and C-Film must be positioned with the coated sides facing each other. These papers are available in two rolls of 10000 (mm) × 270 (mm) × 0.1 (mm) and work in such a way that the red-colored paper contains very small colored microcapsules that contaminate the white paper under received pressure. The paper measurements are 270 × 250 mm and 230 × 220 mm and are placed such that their rough parts are placed on top of each other. Also, two 270 × 1300 mm papers were cut for half of the concrete and wooden sleepers and bonded with paper glue, as can be seen in Figures 3 and 4.

4. Field investigation

Experiments were carried out in the odd track of 18+700 km Aprin-Maleki block in the Tehran-Karaj-Qazvin line. This site was selected due to the need for both types of concrete and wooden sleepers. For installing sensitive pressure papers, the crib and shoulder ballast on both sides of the sleeper are emptied, and the ballast below the sleeper is left intact so that it will not need tamping. The track panel was moved upward in order to place the pressure papers under the sleepers [30]. These papers were placed under two concrete and two wooden sleepers, as shown in Figure 5.

After installing the pressure paper, the crib ballast was filled in. The pressure paper was then subjected to cyclic loading of the trains. This section experienced the passage of freight trains with a total tonnage of 800,000 kN and 6,700 axles, including 85 locomotives with a speed of 80 km/h. The type of the ballast used in this track was basalt, the specifications

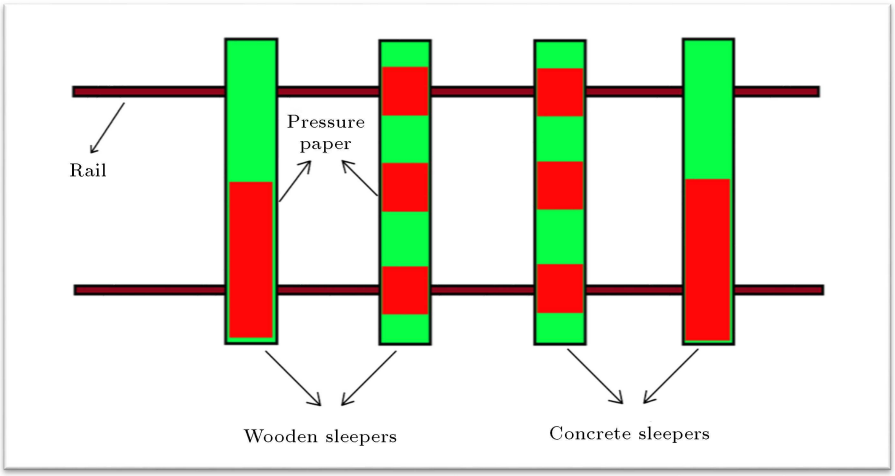

(a)

(b)

Figure 5. (a) Pressure paper installment; (b) Track preparation for tests.

of which are given in the following. After the intended loading was done, the crib and shoulder ballast were emptied again and the pressure papers were removed and scanned. Then, the data of the pressure papers were analyzed using Adobe Photoshop CC 2017 and ImageJ software. An example of image processing for obtaining the amount of surface that has changed its color is shown in Figure 6.

5. Laboratory investigation

In laboratory investigations, the ballast box test was used. The ballast box apparatus was a steel box with the dimensions of 700 mm (l) × 300 mm (w) × 450 mm (h), and the dimensions of the loading plate were 220 × 230 mm. Moreover, the maximum value of cyclic loading frequency was considered as 3 Hz [31]. For this research, the particles of ballasts were filled in the ballast box with the specified grading, and the contact surface measurement paper was placed beneath the hydraulic jack to evaluate the pressure paper. This experiment was performed for different samples to determine the effect of loading and cycles and the effect of ballast particles on the contact surface between sleeper and ballast. Figure 7 shows the images of the ballast box testing device.

To determine the effect of the loading cycle, experiments were performed with different cycles of 6700, 20000, and 50000 for ballast type 1 with the 30 kN load. To determine the effect of the axle load, the experiment was performed on ballast type 1 with axle loads of 30, 37.7, and 45.2 kN under 20000 cycles. This is equivalent to real loads of 200, 250, and 300 kN at a speed of 80 km/h on the real track.

The calculations for 200 kN according to AREMA Manual-2006 are given in Eqs. (1) to (4). In these relations, V is shown in km/h unit and D is the diameter of the wheel in millimeters. In addition, it is assumed that only 50% of the axle load of the train is received by the sleeper exactly under the load:

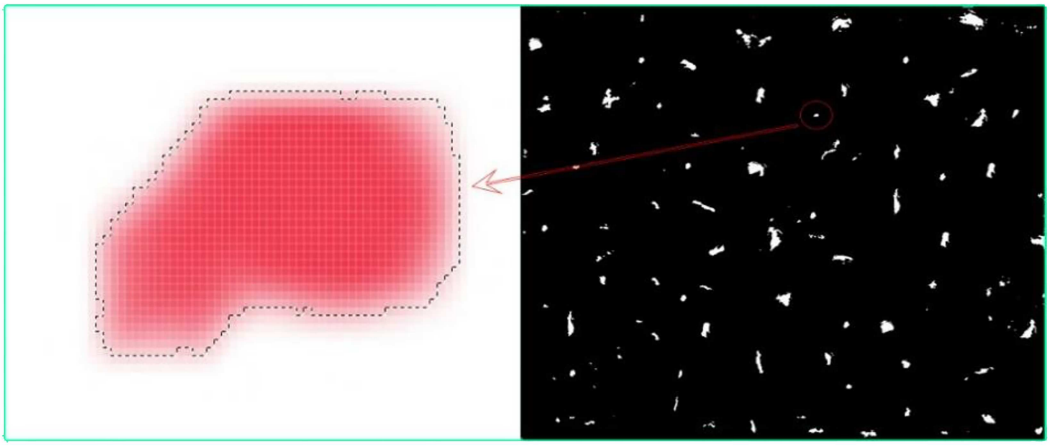

Figure 6. Image analysis with software.

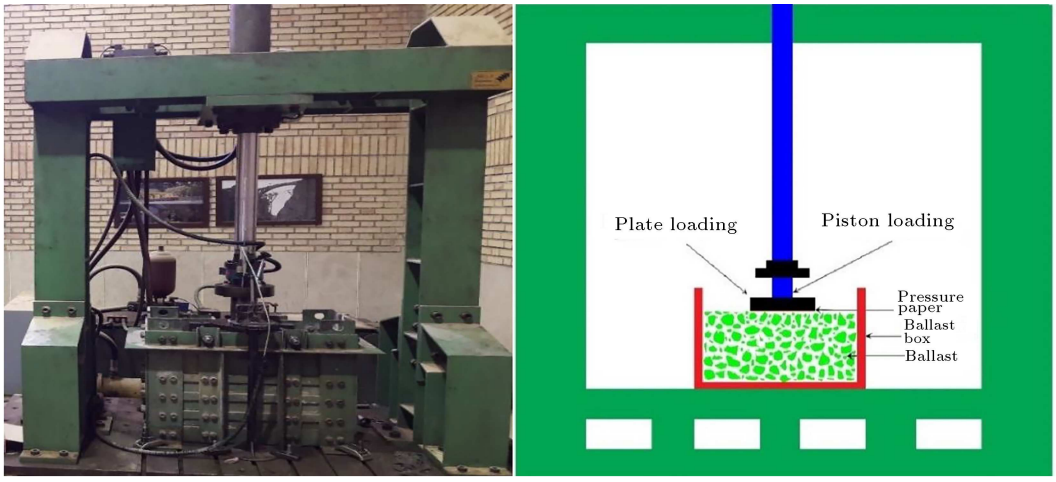

Figure 7. Photo of the box testing device.

$$\varphi = 1 + 5.21\frac{V}{D} = 1 + 5.21\frac{80}{914} = 1.456, \quad (1)$$

$$P_d = \varphi * \frac{P_s}{2} = 1.456 * \frac{200}{2} = 145.6 \text{ kN}, \quad (2)$$

$$\sigma = \frac{P}{A} = \frac{145.6(\text{kN})}{1.22 * 0.2} = 596.7 \text{ (kN/m}^2\text{)}, \quad (3)$$

$$P_{ballast\ box} = \sigma * A_{ballast\ box} = 596.7 * 0.22 * 0.23 \simeq 30 \text{ (kN)}, \quad (4)$$

φ Dynamic impact factor
V Speed(km/h)
D Wheel diameter (mm)
P_d Dynamic force
P_s Static force
σ Stress

For investigating the effect of ballast type on the contact area between sleeper and ballast, experiments were conducted on three different types of ballast with 20000 cycles and 30 kN axle load. This test includes ballasts of types 1 and 4 and ballast samples from the test site. For investigating the effect of USP, two types of stiff and soft pads were used, the technical specifications of which are shown in Table 4 and Figure 8.

Table 4. Specifications of USP used.

Soft USP	Stiff USP	Property
SLS 1308 G	SLB 3007 G	Technical ID
8	7	Thickness (mm)
70	30	Weight (N/m^2)
0.13	0.3	Stiffness (N/mm^3)

6. Results

Table 5 shows the characteristics of the tested ballast. Ballasts of types 1 and 4 are compliant with code 301, and the specifications of the sample ballast from the field are between types 1 and 4, bing acceptable [32].

Figure 8. The Under Sleeper Pads (USP) used in this experiment.

Table 5. Ballast grading.

Standard sieves									
#4	3/8	1/2	3/4	1	3/2	2	5/2	3	Grading
–	–	2.5	10	–	42.5	–	95	100	Type 1
–	0	–	5	20	75	95	100	–	Type 4
0	0.36	3.81	12.74	21.31	50.98	87.48	100	100	Field

Table 6. Tests on ballast sample.

Row	Test name	Test result	Limit value	Assessment's result
1	Determining the material circularity [33]	1.56%	5%	✓
2	Determination of water absorption percentage of aggregates	0.81%	1%	✓
3	Grains with broken surfaces [34]	5.10%	10%	✓
4	Grain shape factor	2.11	–	✓
5	The amount of spherical material	0.33%	5%	✓
6	Percent of long grains	10.7%	30%	✓
7	Flakiness index [35]	4.56%	5%	✓
8	Potential for crushing aggregates	12.84%	50%	✓
9	Impact test	3.26%	10%	✓
10	Los angeles abrasion test	16.5%	30%	✓

To illustrate the characteristics of the ballast used in the case study of this paper, the results of experiments performed on the field ballast sample are shown in Table 6.

6.1. Field test results

As shown in Figure 9(a) and (b), due to the lower elasticity of the concrete sleeper, the contact area between the sleeper and the ballast particles was low and the average contact surface area reached 4.9%. In Figure 9(a), the pressure paper was placed under two rail seats and the middle of the sleeper.

Also, in Figure 9(b), the pressure paper was placed under half of the sleeper. However, as shown in Figure 10(a) and (b), the wooden sleeper has a higher contact surface with ballast particles due to its higher elasticity than the concrete sleeper and the average contact surface area reached 8.1%. In Figure 10(a), the pressure paper was placed at three points of the wooden sleeper (below two rail seats and the middle of the sleeper), and in Figure 10(b), the pressure paper was placed under half of the sleeper and then, was mirrored for the other half.

Of note, the distribution of the contact surface is different under different parts of concrete and wood sleepers, as shown in Figure 11(a) and (b). In this

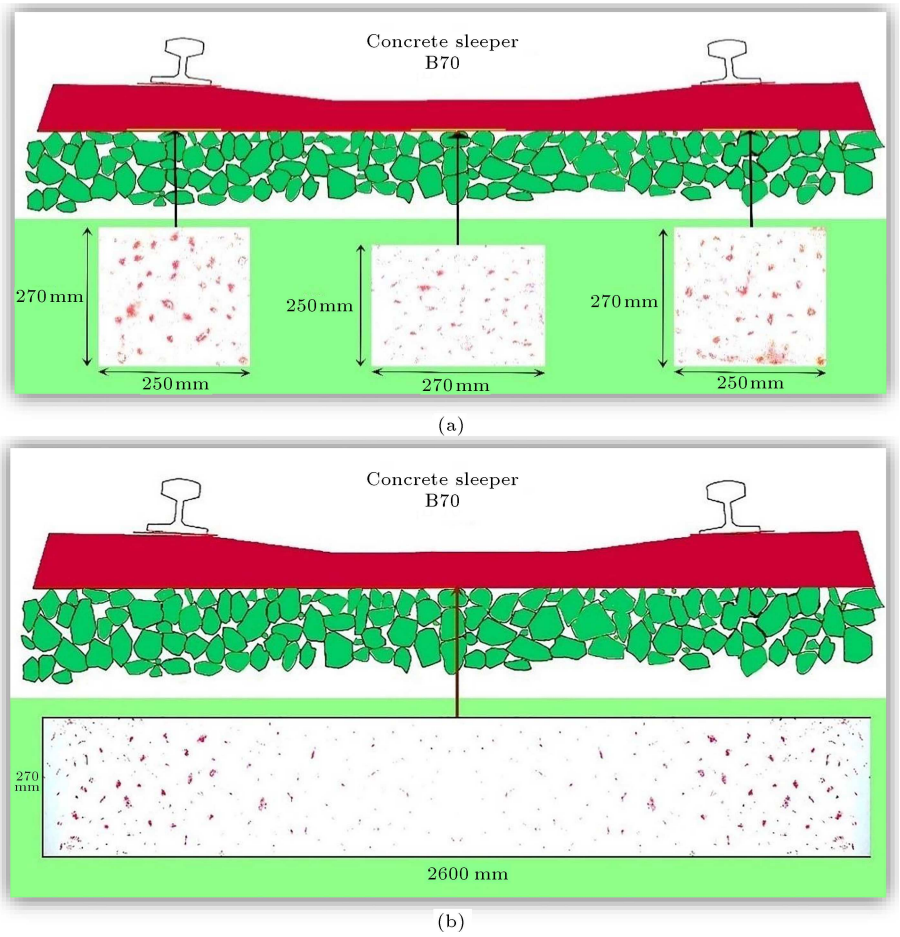

Figure 9. An image of the results of the pressure papers under the concrete sleeper.

figure, the wooden and concrete sleepers are divided into different parts, and the amount of contact area between the sleepers and the ballast is calculated in different sections. According to the results, for different parts of the sleeper, it was observed that the highest level of contact occurred below the rail seats, while the contact area in the middle of the sleeper was the lowest.

6.2. Distribution of forces under the sleeper

The following method was employed to calculate the stresses and forces applied to the sleeper by assuming a uniform distribution of the force between the wheels on a single axle. For example, the widespread load under concrete sleeper was calculated according to Eqs. (5) and (6), and its results are shown in Figure 12(a):

$$\sigma = \frac{P}{A} = \frac{\frac{1}{2} * 200 \text{ (kN)}}{\frac{4.91}{100} * 2600 * 274.2 \text{ (mm)}} = 2.857 \frac{\text{N}}{\text{mm}^2}, \quad (5)$$

$$P_i = \sigma_i * L_i \Rightarrow P = 2.857 * \left(\frac{4.03}{100} * 274.2\right) = 31.6 \frac{\text{N}}{\text{mm}}. \quad (6)$$

Thus, the distributed forces beneath the sleeper were obtained. Moreover, these calculations apply to the second half of the sleeper as well as the first half. Figure 12(a) and (b) shows the distribution of forces beneath concrete and wooden sleepers.

6.3. Results of ballast box tests

For comparing the results of the ballast box test with the field test, a ballast sample from the field test site was used. This ballast experienced 6700 cycles of loading with the value of 30 kN (equivalent to 200 kN on-site), and the contact surface was compared with the field results with a conversion factor of 1.86. This coefficient was utilized to equate field and laboratory conditions:

$$Conversion\ factor = \frac{Contact\ surface\ at\ the\ field\ test\ (\%)}{Contact\ surface\ in\ the\ laboratory\ (\%)} = \frac{4.91\%}{2.64\%} = 1.86. \quad (7)$$

Below are the results obtained from the ballast box test:

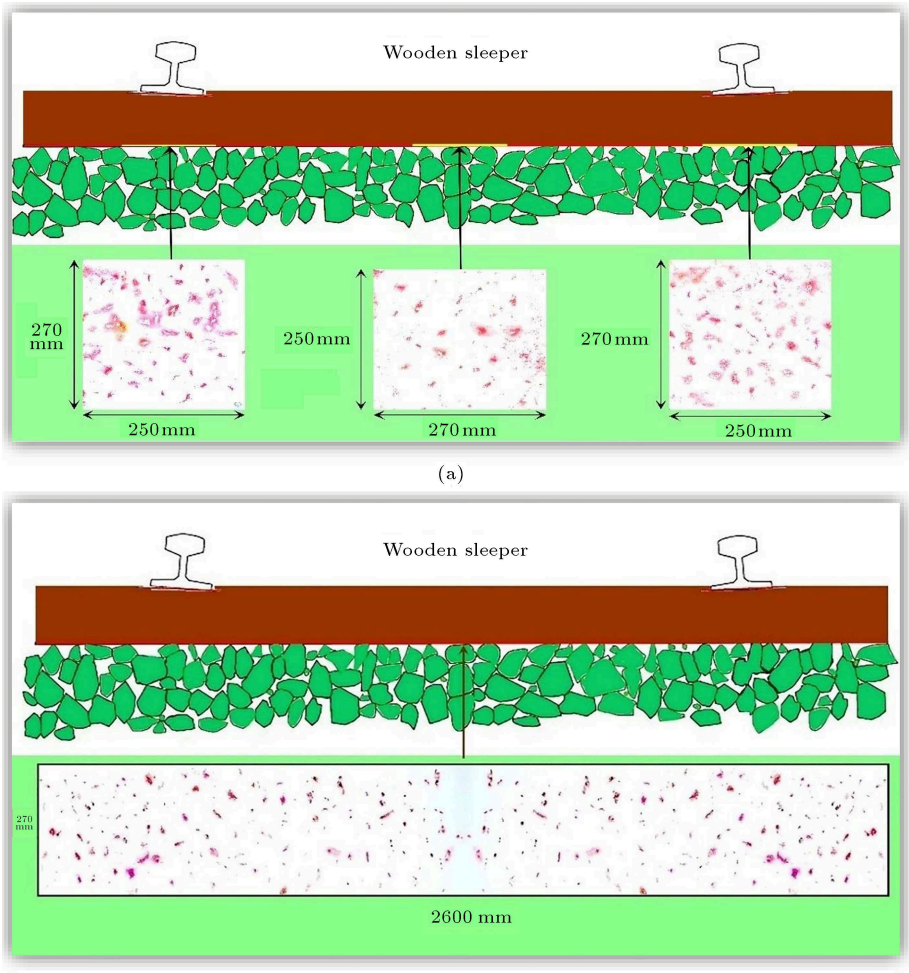

Figure 10. An image of the results of the pressure papers below the wooden sleeper.

- **Effect of the ballast:** As shown in Figure 13, the ballast type is effective in the contact surface between the sleeper and the ballast. Moreover, the finer ballast particles result in a higher contact surface between the sleeper and the ballast. The average contact areas for ballast types 1 and 4 were 4.6% and 5.5%, respectively, while this value was 5.3% for ballast samples from the field test site;
- **Effect of the loading cycle:** As shown in Figure 14, the loading cycle has affected the contact surface between the sleeper and ballast. Moreover, as the cycles increase, the contact area between the sleeper and ballast particles increases; however, this increase has continued to some extent and remained almost constant afterward. The reason for the small difference between 20,000 and 50,000 cycles is that over time and numerous cycles, the amount of contact surface remains almost constant and does not change significantly. The average contact area for 6700, 20000, and 50000 cycles is 4.2%, 4.6%, and 4.7%, respectively;
- **Effect of the load:** As shown in Figure 15, the axle load is effective in the contact surface between the sleeper and ballast, and as the applied load increases, the contact area increases. The average contact surface for 30, 37.7, and 45.2 kN is 3.8%, 4.5%, and 5.1%, respectively;
- **Effect of (USP):** As can be seen in Figure 16, using pads is very effective in the contact surface between the sleeper and ballast, and the softer pads result in a higher contact area. The average contact surface for ballasts of type 1 without pads is 4.6%, while for stiff type pads, it is 15.9% and for soft type pads, it is 21.6%. It has been observed that USP increases the contact surface between the sleeper and ballast and distributes wheel load between more ballast areas.

The results of all the above experiments are summarized and presented in Table 7.

The experiments were performed for different samples to determine the effect of loading value, applied cycles, the effect of USP, and the effect of ballast particle's type on the contact surface between the

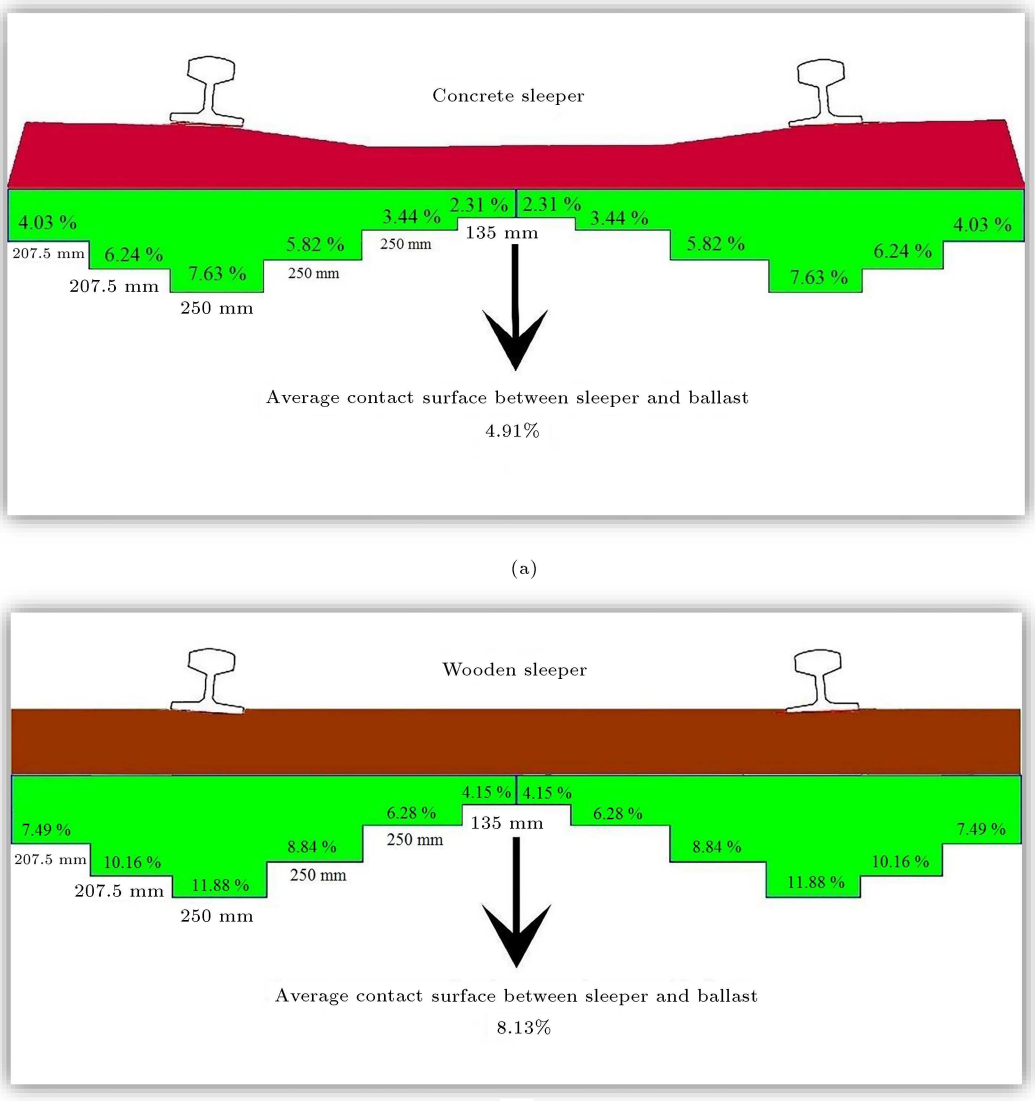

Figure 11. (a) Schematic spectacle of concrete sleeper; (b) Schematic show of wooden sleeper.

sleeper and ballast. The results were compared to that of another study and it was found that contact area rates were approximately higher than 1%, which was acquired at the University of Southampton. Therefore, it is likely that their laboratory condition be different from the actual conditions of the track. These rates are lower than those in McHenry's work, being about 16 to 30%. These results show that the stress distribution under the sleeper is completely non-uniform, and the area under the rails has the highest stress while the least stress is under the middle of the sleeper. However, with the passage of time and cyclic loads, this distribution tends to become uniform and to solve this problem, tamping is needed to be done on tracks.

The difference between the results of this study and those of Abadi et al. [27] is that despite the use of one type of pressure paper, they may have misinterpreted the calculations and analyses of the images given in their paper and obtained lower values since the numbers and percentages obtained by their research did not match the red-colored photos of the pressure papers, showing a higher contact area. However, the difference between the results of this study and those of McHenry at the University of Kentucky is that he used a rubber layer at the top and bottom of the sensor to prevent the creation of holes in surface sensors. Also, this rubber layer acts like an USP and increases the value of the contact area. According to the results of this study, for ballast type 1 and using USP, the values are 21.6% for soft type pads and 15.9% for stiff type pads, while the results of McHenry study for the new ballast show that the numbers are close and this is due to their use of the rubber layer above and below the contact surface measurement sensor.

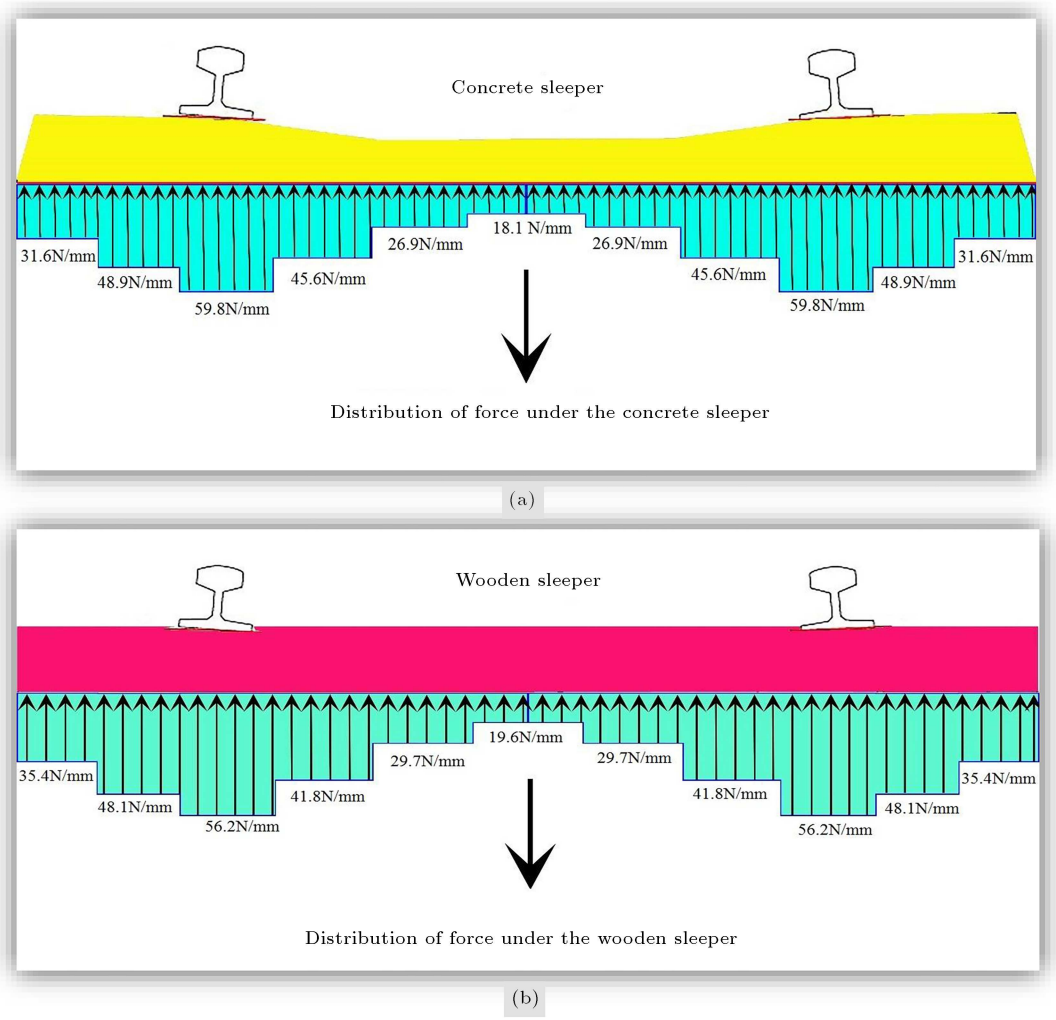

Figure 12. (a) Distribution of forces under concrete sleeper; (b) Distribution of forces under wooden sleeper.

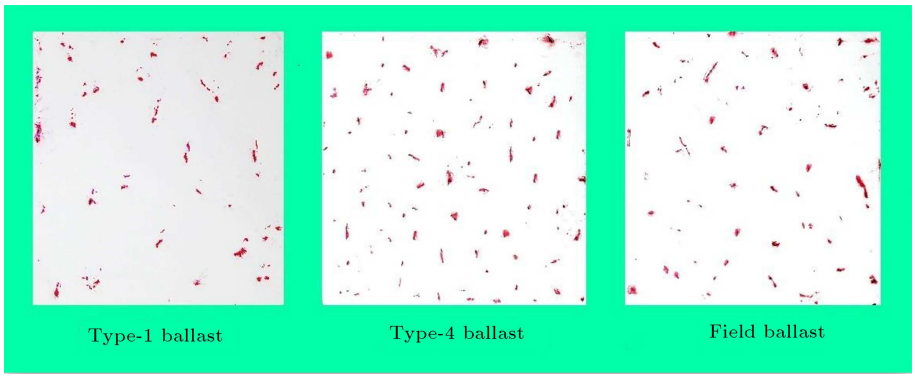

Figure 13. Effect of ballast type on contact surface between sleeper and ballast.

7. Conclusion

The contact surface and stress distribution beneath the sleeper were not uniform since they reached their peak under the rails. The low contact surface of ballast particles with sleepers may cause fracture and abrasion. In this study, both field and laboratory tests were performed for accuracy, and more accurate results were obtained from previous studies. The field experiments found that wooden sleepers had a higher contact surface than concrete sleepers, and the effective contact surfaces between sleepers and ballast particles for concrete and wooden sleepers were 4.9% and 8.1%, respectively. This result indicated that the wooden

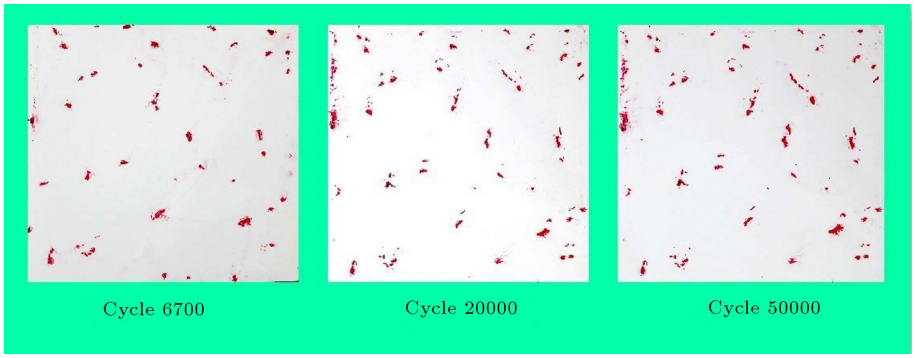

Figure 14. The effect of the loading cycle on the contact surface between the sleeper and the ballast.

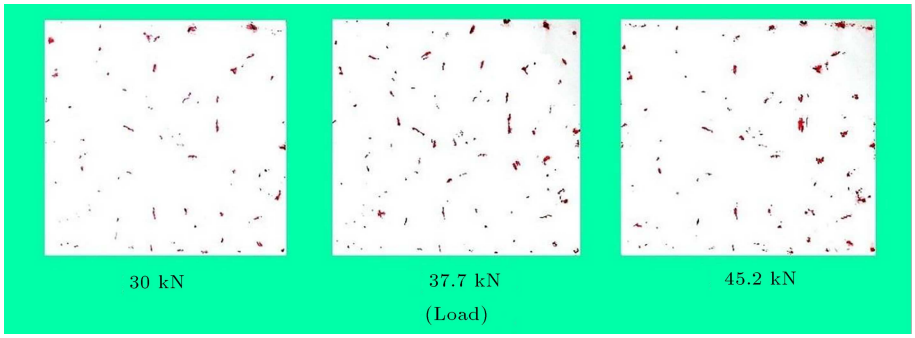

Figure 15. The effect of axle load on the contact surface between the sleeper and the ballast.

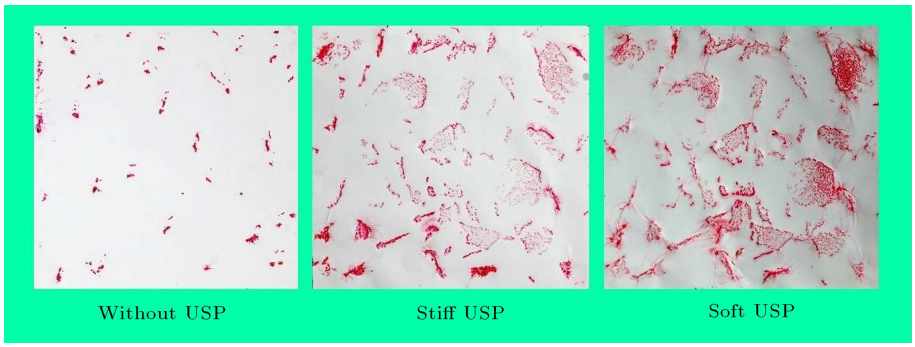

Figure 16. The effect of the USP on the contact surface between the sleeper and the ballast.

sleeper had a higher contact surface due to its lower rigidity and higher elasticity and this, therefore, is a reasonable result.

The results obtained for the ballast box testing showed that the type of ballast was effective in the contact surface between the sleepers and ballast and fine-grading particles tended to have a higher contact surface. As a result, the type-4 ballast had a higher contact surface than the type-1 ballast. Ballast samples from the field had more contact surface than type 1 and lower contact surface than the ballast type 4. In these experiments, it was observed that as the loading cycle increased, the amount of contact surface increased. Still, this increase remained almost constant after a while, and its changes were negligible. Also, the contact surface between the sleepers and ballast was directly affected by the amount of loading.

In this research, it was found that the use of Under Sleeper Pad (USP) greatly increased the contact surface between the sleepers and ballast and transferred the trainload between a higher surface of the ballast layer, which reduced stresses under the sleeper and prevented sleeper cracking, ballast abrasion, and crushing. The following items can be done to increase the amount of effective contact surface between the sleepers and ballast:

- Better grading of ballast, which includes using a layer of better material under the sleeper;
- USPs with softer USPs since they yield the most increase;
- Using less rigid sleepers such as wooden or plastic sleepers;

Table 7. Summary of results from field and laboratory experiments.

Type of experiment	Test specifications	Contact surface (%)	Total surface value pressure paper (mm^2)	Color surface value (mm^2)	Average compressive stress (MPa) $\frac{F_{max}}{A_{CONTACT}}$
Field experiment	Concrete sleeper	4.9	713000	35020	2.8
	Wooden sleeper	8.1	702000	57090	1.75
Laboratory testing (ballast box)	6700 cycle	4.2	55200	2320	6.5
	20000 cycle	4.6	55200	2540	5.9
	50000 cycle	4.7	55200	2590	5.8
	Ballast type 1	4.6	55200	2540	5.9
	Ballast type 4	5.5	55200	3040	4.9
	Sample ballast field	5.3	55200	2920	5.1
	30 kN load	3.8	55200	2100	7.1
	37.7 kN load	4.5	55200	2480	6
	45.2 kN load	5.1	55200	2810	5.3
	USP soft	21.6	55200	11920	1.3
	USP stiffness	15.9	55200	8780	1.7

- Using a frame or half-framed sleeper to increase the contact surface below the rail seat.

References

1. Song, W., Huang, B., Shu, X., et al. "Interaction between railroad ballast and sleeper: a DEM-FEM approach", *International Journal of Geomechanics*, **19**(5), pp. 15–32 (2019).
2. Abadi, T., Pen, L.L., Zervos, A., et al. "Effect of sleeper interventions on railway track performance", *J. Geotechnical and Geoenvironmental Engineering*, **145**(4), 04019009 (2019).
3. Navaratnarajah, S.K., Indraratna, B., and Ngo, N.T. "Influence of under sleeper pads on ballast behavior under cyclic loading: Experimental and numerical studies", *Journal of Geotechnical and Geoenvironmental Engineering*, **144**(9), 04018068–16 (2018).
4. Indraratna, B. and Salim, W., *Mechanics of Ballasted Rail Tracks, a Geotechnical Perspective*, 1st, Edition, London, UK, Taylor & Francis Group plc (2005).
5. Esveld, C., *Modern Railway Track*, 2nd Edition, MRT-Productions, The Netherlands (2001).
6. Selig, E.T. and Waters, J.M., *Track Geotechnology and Substructure Management*, 1st Edition, Thomas Telford, London, UK (1994).
7. Lichtberger, B. "The lateral resistance of the track", (Part2), European Railway Review, pp. 68–71 (2007).
8. Talbot, A.N. "Stresses in railroad track", The Second Progress Report of the ASCE-AREA Special Committee on Stresses in Railroad Track, Reprinted, Published by the American Railway Engineering Association (AREA) (1919).
9. Guo, Y., Jia, W., Markine, V., et al. "Rheology study of ballast-sleeper interaction with Particle Image Velocimetry (PIV) and Discrete Element Modelling (DEM)", *Construction and Building Materials*, **282**(5), 122710 (2021).
10. Jing, G.Q., Aela, P., and Fu, H. "Numerical analysis of ballast-TDA mixture under cyclic loading", *Proceedings of the Inaugural World Transport Convention Beijing*, China, June 4–6 (2017).
11. Liu, S., Huang, H., Qiu, T., et al. "Comparison of laboratory testing using smart rock and discrete element modeling of ballast particle movement", *Journal of Materials in Civil Engineering*, **29**(3), p. 1061 (2017).
12. Ji, S., Sun, S., and Yan, Y. "Discrete element modeling of dynamic behaviors of railway ballast under cyclic loading with dilated polyhedral", *Int. J. Numer. Anal. Meth. Geomech*, **41**(2), pp. 180–197 (2017).
13. Ferro, E., Harkness, J., and Le Pen, L.J.T.G. "The influence of sleeper material characteristics on railway track behaviour:concrete vs composite sleeper", *Transportation Geotechnics*, **23**(6), 100348 (2020).
14. Guo, Y., Wang, J., Markine, V., et al. "Ballast mechanical performance with and without under sleeper pads", *KSCE Journal of Civil Engineering*, **24**(11), pp. 3202–3217 (2020).
15. Li, H. and McDowell, G.R. "Discrete element modelling of under sleeper pads using a box test", *Granular Matter*, **20**(2), pp. 1–12 (2018).
16. Jayasuriya, C., Indraratna, B., and Ferreira, F.B. "The use of under sleeper pads to improve the performance of rail tracks", *Indian Geotech Journal*, **50**(2), pp. 204–212 (2020).
17. Zakeri, J.A. and Sadeghi, J. "Field investigation on load distribution and deflections of railway track sleep-

ers", *Journal of Mechanical Science and Technology*, **21**(12), pp. 1948–1956 (2007).

18. Profillidis, V. and Poniridis, P. "The mechanical behavior of the sleeper-ballast interface", *Computers & Structures*, **24**(3), pp. 437–441 (1986).
19. Henn, W. "Auswirkung von Oberbauform und Betriebsbelastung auf die Veranderung der Gleishohenlage", *ARCH. EISENBAHNTECH.*, DEU, **33**, pp. 51–64 (1978).
20. Sysyn, M., Przybylowicz, M., Nabochenko, O., et al. "Mechanism of sleeper-ballast dynamic impact and residual settlements accumulation in zones with unsupported sleepers", *Sustainability*, **13**(14), p. 7740 (2021).
21. Jing, G., Aela, P., and Fu, H. "The contribution of ballast layer components to the lateral resistance of ladder sleeper track", *Construction and Building Materials*, **202**(3), pp. 796–805 (2019).
22. Jing, G., Ji, Y., and Aela, P. "Experimental and numerical analysis of anchor-reinforced sleepers lateral resistance on ballasted track", *Construction and Building Materials*, **264**(12), p. 120197 (2020).
23. De Iorio, A., Grasso, M., Penta, F., et al. "On the ballast-sleeper interaction in the longitudinal and lateral directions", *Proceedings of the Institution of Mechanical Engineers, Part F: Journal of Rail and Rapid Transit.*, **232**(2), pp. 620–631 (2018).
24. Pucillo, G.P., Penta, F., Catena, M., et al. "On the lateral stability of the sleeper-ballast system", *Procedia Structural Integrity*, **12**(1), pp. 553–560 (2018).
25. Ngamkhanong, C., Feng, B., Tutumluer, E., et al. "Evaluation of lateral stability of railway tracks due to ballast degradation", *Construction and Building Materials*, **278**(4), p. 122342 (2021).
26. McHenry, M.T. "Pressure measurement at the ballast-tie interface of railroad track using matrix based tactile surface sensors", University of Kentucky, Theses and Dissertations - Civil Engineering (2013).
27. Abadi, T., Le Pen, L., Zervos, A., et al. "Measuring the contact area and pressure between the ballast and the sleeper", *The International Journal of Railway Technology*, **4**(2), pp. 45–72 (2015).
28. Sadeghi, J., *Fundamentals of Analysis and Design of Railway Ballasted Track*, 1st Edn., pp. 57–130, IUST press, Tehran, Iran (2018).
29. Fuji Film "Fuji film prescale pressure measurement film", Available: https://www.fujifilm.com/sg/en/business/inspection/measurement-film/prescale/feature (2018).
30. Refahiat Nikoo, H.R. "Field and laboratory investigation on the effective contact surface between sleeper and ballast particles in railway track", MSc Theses in Railway Engineering, Iran University of Science and Technology (2019).
31. Esmaeili, M., Aela, P., and Hosseini, A. "Experimental assessment of cyclic behavior of sand fouled ballast mixed with tire derived aggregates", *Soil Dynamics and Earthquake Engineering*, **98**(7), pp. 1–11 (July, 2017).
32. Iranian Railway-Code 301, *Railway Track Super Structure General Technical Specification*, "General-technical properties of ballasted railway track", Publications of the Organization of Management and Planning of the Country 84/00/67, p. 80 (2005).
33. *British Standard Institution, British Standard Institution BS EN 13450:2002*, Aggregates for railway ballast (2002).
34. *British Standard Institution, British Standard Institution BS EN 933-5:1998*, Tests for geometrical properties of aggregates. Part 5: Determination of percentage of crushed and broken surfaces in coarse aggregate particles (1998).
35. *British Standard Institution, British Standard Institution BS EN 933-3:2012*, Tests for geometrical properties of aggregates. Part 3: Determination of particle shape, Flakiness index (2012).

Biographies

Hamidreza Refahiat-Nikoo received his MSc degree in Railway Engineering from Iran University of Science and Technology, Tehran, Iran in 2019. His research interests include analysis of railway tracks and track maintenance and construction.

Jabbar-Ali Zakeri received his PhD degree in Road and Railway Engineering from Beijing Jiaotong University, China in 2000. Dr Zakeri is currently a Professor at the School of Railway Engineering, Iran University of Science and Technology. His research interests include dynamic analysis of train-track interaction, railway track dynamics, and track maintenance and construction.

Saeed Mohammadzadeh received his PhD degree in Structural Engineering from Iran University of Science and Technology, Iran in 2002. Dr Mohammadzadeh is currently an Associate Professor at the School of Railway Engineering, Iran University of Science and Technology. His research interests include railway track dynamics, test and empirical analysis of track and structures, optimization and reliability analysis, and maintenance and repairing management.